View metadata, citation and similar papers at core.ac.uk

brought to you by CORE

provided by Loughborough University Institutional Repository

Loughborough University

This item is distributed via Loughborough University's Institutional Repository (https://dspace.lboro.ac.uk/) and is made available under the following Creative Commons Licence conditions.

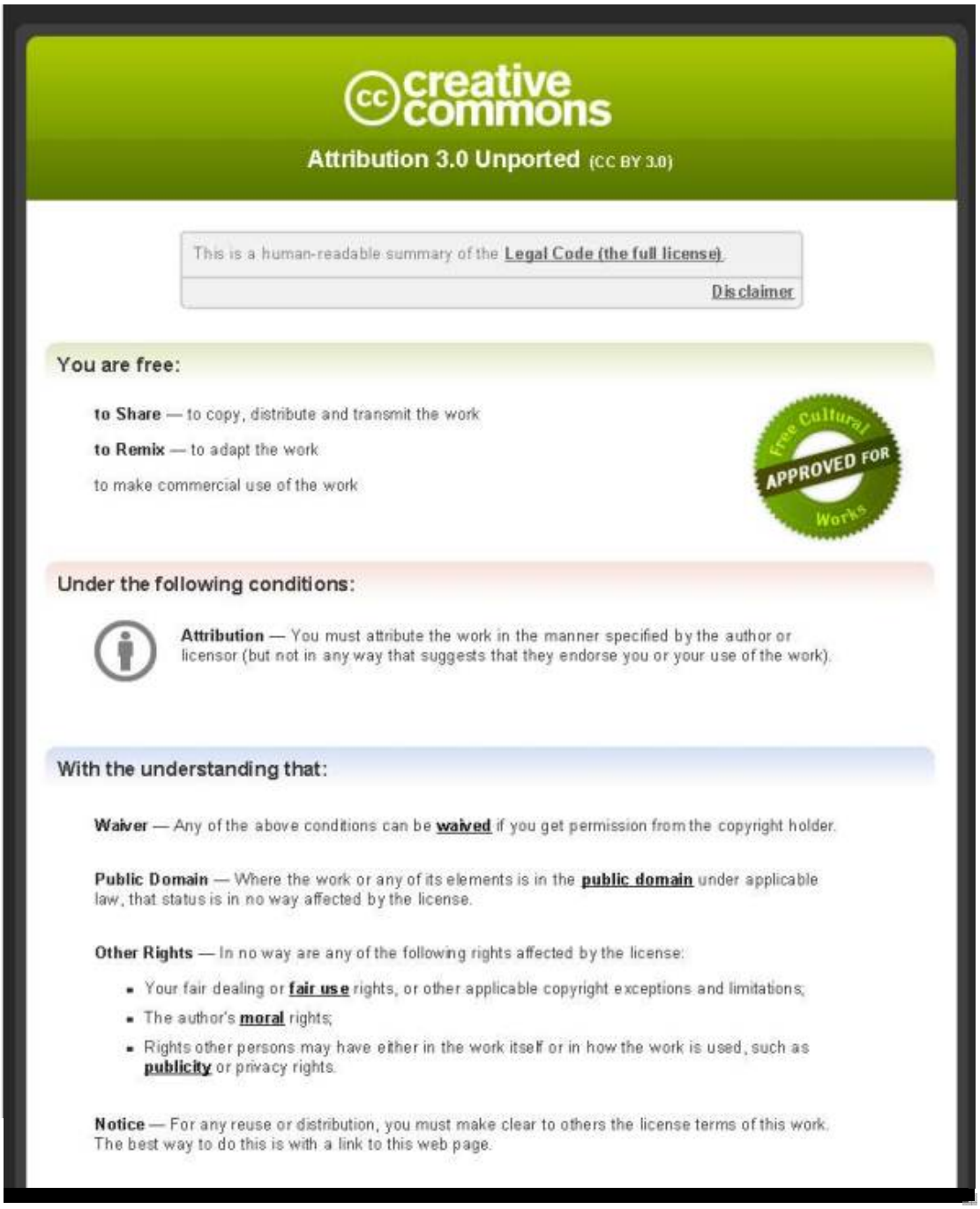

For the full text of this licence, please go to:
http://creativecommons.org/licenses/by/3.0/

Applied Mathematical Modelling 37 (2013) 406–419

Contents lists available at SciVerse ScienceDirect

Applied Mathematical Modelling

journal homepage: www.elsevier.com/locate/apm

Thin film tribology of pharmaceutical elastomeric seals

D.W. Grimble [a], S. Theodossiades [a,*], H. Rahnejat [a], M. Wilby [b]

[a] Wolfson School of Mechanical and Manufacturing Engineering, Loughborough University, Loughborough, UK
[b] 3M Drug Delivery Systems, 3M Health Care Ltd., Loughborough, UK

ARTICLE INFO

Article history:
Received 22 April 2011
Received in revised form 6 February 2012
Accepted 29 February 2012
Available online 8 March 2012

Keywords:
Pressurised metered dose inhaler
Elastomeric pharmaceutical seals
soft Ehl
Siliconisation

ABSTRACT

The primary purpose of valve seals in inhalation and other drug dispensing devices is to inhibit leakage of highly volatile formulation from pressurised canisters. This requirement often conflicts with smooth operation of valves because of poor lubrication of seals. The repercussions of this can be variability in dispensed dose as well as loss of prime and gradual wear of seals. Although a good volume of literature is available for general purpose o-ring seals, the characteristic behaviour of those used in pharmaceutical devices deviate from this significantly. The paper studies tribology of such seals, subjected to global fitment and canister pressure deformation and localised conjunctional elastohydrodynamic pressures. It is shown that ideally smooth seals would operate under iso-viscous elastic (*soft EHL*) regime of lubrication. However, the predicted ultra-thin films are insufficient to ensure fluid film lubrication because of rough micro-scale nature of elastomeric seal surface and poor lubricity of the usual bio-compatible formulations. The paper also shows that siliconisation of elastomeric contacting surface only marginally improves its tribological performance.

© 2012 Elsevier Inc. All rights reserved.

1. Introduction

Many inhalation devices contain drug formulations (mixtures) which are volatile and kept in metering chambers under pressure. Sealing of the chamber is a primary design requirement. Smooth actuation of the device is also an important design attribute, which can often conflict with its primary sealing requirement. This calls for the use of a bio-compatible lubricant, a desired property of the propellant which accounts for the main constituent of the mixture. This is the characteristic of chlorofluorocarbon (CFC), which was abandoned after its undesired effect upon the ozone layer was recognised. Instead many inhalation devices now use hydrofluoroalkane (HFA)-based propellants which interact minimally with the surfaces of the chamber and the seals because of its inert nature [1]. HFA, however, suffers from very poor lubricity. As the result, the elastomeric seals for pharmaceutical device applications are often furnished with a film of silicone oil (a process referred to as siliconisation). With HFA being the propellant of choice, only certain types of elastomeric seals may be used. Thus, in a variety of applications where elastomers are the main sealing elements, such as pressurised metered dose inhalers (pMDIs) and syringes, the seal performance represents the main contributory factor to the overall system friction. Whilst reducing friction is a desired outcome, it should not compromise the primary sealing function.

It is only recently that some research effort has been directed towards tribology of elastomeric seals in pharmaceutical devices [2,3]. However, research into pharmaceutical seals inherits a larger volume of general research on seal tribology. One key issue has been the prediction of contact pressure distribution and thus the conjunctional load in order to assess

* Corresponding author.
E-mail address: s.theodossiades@lboro.ac.uk (S. Theodossiades).

0307-904X/$ - see front matter © 2012 Elsevier Inc. All rights reserved.
http://dx.doi.org/10.1016/j.apm.2012.02.035

Nomenclature

b	width of effective seal contact
c	seal undeformed half face-width
D	seal cross-sectional diameter (undeformed)
E	elastic modulus of EPDM rubber
E_p	elastic modulus of Polybutylene Terethalate
E'	equivalent elastic modulus of the contact
h	film thickness
h_0	minimum film thickness (rigid gap)
H	dimensionless film thickness
H_0	dimensionless minimum film (gap)
i	position along the face-width where deflection is calculated
j	an iteration counter
k	position of a pressure element
l	perimeter of the seal
n	number of discrete computational elements
p	elastohydrodynamic contact pressure
P	load per unit computational element width
P_H	equivalent Hertzian pressure
p^*	dimensionless contact pressure
R	cross-sectional seal radius
R_1	radius of the undeformed seal before fitment
R_2	radius of the rectangular groove
R_{zy}	equivalent radius of contact
S	face-width profile of the seal
u	speed of lubricant entraining motion
w	contact load
U^*	dimensionless speed parameter (rolling viscosity parameter)
W^*	dimensionless load parameter
x	normal to the seal cross-section
y	along the seal face-width
Y_e	exit boundary (Film rupture point)
Y_i	inlet meniscus
z	along the cross-section of the seal
α	pressure viscosity coefficient of lubricant
β	relaxation constant for fitment load per unit length
χ	under relaxation factor for elasto-hydrodynamic pressures
δ	localised deflection of the seal
Δ	global seal deflection due to fitment and canister pressure
$\bar{V}$	dilatation
ε_f	error in fitment extension
ε_{p^*}	error in elastohydrodynamic pressure convergence
ε_y, ε_z	cross-sectional strains
γ	shear strain
η	dynamic viscosity at contact pressure
η_0	dynamic viscosity at atmospheric pressure
ρ	density at contact pressure
ρ_0	density at ambient pressure
σ_y, σ_z	principal stresses
τ_{zy}	shear stress
υ	Poisson's ratio for EPDM rubber
υ_p	Poisson's ratio for Polybutylene Terethalate
ζ	damping factor for convergence of lubricant reaction

sealing effectiveness. The first step in this process is the accurate prediction of contact geometry when a seal is fitted *in situ* and is subjected to a differential pressure.

The initial approaches involved use of Hertzian theory for o-ring seals to represent their localised deformation in one dimensional analysis, when they are loaded against their retaining grooves. However, Hertzian theory does not take into

account the large strain global seal deflection during fitment. Muskhelishvili [4] solved the first and second fundamental problems of a circular disk (o-ring cross section) under concentrated forces applied to its boundary (based on the works of Michell [5] and Love [6]). The first problem was the calculation of the elastic equilibrium of a body, if the external stresses or forces acting on its boundaries are given, while the second problem is to calculate the elastic equilibrium when the displacements of the boundary points are given.

Lindley [7] investigated the load-compression characteristics of toroidal elastomeric seals. His approach focused on the seal deflection due to fitment/compression. An analytical method was developed, where the localised Hertzian deflection was coupled with an empirically determined modification to account for the large fitment strains in compression. The work showed reasonable agreement with experimental results for moderately deformed seals. However, George et al. [8] showed that as strain levels increased, progressively the results of Lindley's approach underestimated the extent of deformation. In George et al. [8] an FEA approach was undertaken, which showed no discernible difference with the basic analytical approach of Lindley [7] until the seal compressive strain exceeded 20% of its cross-sectional depth.

Dragoni and Strozzi [9] reviewed the case of a laterally restrained o-ring within a rectangular groove under compressive loads. They ignored the effect of sealing pressure. An FEA approach included a suitable mesh to cover the o-ring cross-section, assuming the seal to be approximated by a disk of unit thickness. A further modification was presented to account for the restraining walls of the groove. Green and English [10,11] expanded the work of Lindley [7] and that of Dragoni and Strozzi [9], using FEA for examination of a seal under differing regional contact stresses. The problem of o-ring sealing and deformation was recently revisited by Kim et al. [12], using a mixture of experimental verification and FEA, coupled with the original approach of Lindley [7]. It was shown that the application of a Hertzian pressure distribution profile on seal contacts is a reasonable approach. Furthermore, it was shown that linear elastic approach would be valid for fractional compressions of the cord diameter up to 30%, providing that the ratio of the seal cross-section over the contact width would not exceed a value of 5.

Karaszkiewicz [13–15] investigated the hydrodynamic lubrication of elastomeric o-ring seals, assuming Hertzian contact between the seal and its retaining groove. Using an empirical approach, he calculated the effective contact width of an *in situ* seal subjected to Hertzian contact pressures, augmented by a pressure differential acting across the seal. He noted agreement between his simple hybrid approach and the FEA work of George et al. [8]. He then obtained load per unit length of contact. With the evaluated load and an assumed speed of entraining motion, he employed Hamrock and Dowson [16] extrapolated oil film thickness equation for line contact geometry under soft elastohydrodynamic conditions to predict the lubricant film thickness, allowing for an assumed leakage rate [15]. His method assumes that a coherent film of lubricant is formed in the seal-sliding plunger/stem conjunction. This assumption does not hold true for rough elastomeric seals in drug delivery devices such as inhaler valves as the propellants such as HFA (hydrofluoroalkane) or an applied layer of silicone oil do not form a film of sufficient thickness to guard against direct interaction of surfaces.

Grimble et al. [2] showed that the predominant regime of lubrication for pharmaceutical seals is boundary. Using a friction model, based on the work of Greenwood and Tripp [17], Grimble et al. [2] obtained an estimate of the hysteretic losses in cyclic actuation and release of an inhaler valve. The results conformed well to identical physical conditions using valve compression and release tests. In fact, a detailed characterisation of rough inhaler valve seal surfaces, followed by an analytical model combining viscous friction of a drug formulation, asperity adhesive and deformation frictions by Prokopovich et al. [18] for other variants of inhaler valves confirmed the overall findings of Grimble et al. [2]. With wet seals, Karaszkiewicz [15], Grimble et al. [2], and Prokopovich et al. [18] used the aforementioned extrapolated oil film thickness equation of Hamrock and Dowson [16] to predict the thickness of any lubricant film. This approach renders an analytical solution. However, numerical solutions have also been used for some time now. For example, Hooke et al. [19] incorporated lubrication without the need to resort to a full FEA model for an isotropic elastic o-ring seal in a radial sealing orientation. This was achieved through evaluation of elastic distortion of a circular cross-section with the seal deflection obtained using the general elasticity theory as outlined by Milne-Thomson [20]. This approach assumed a plane strain simplification, similar to that of Lindley [7]. The method also showed reasonable agreement with experimental measurements.

There have been more detailed lubrication studies of o-ring seals in hydraulic actuators, because unlike the elastomeric seals in inhalation devices, elastohydrodynamic conditions have been noted in these cases. Öngün et al. [21] described an axi-symmetric FEA model, the predictions of which showed a prevalent mixed regime of lubrication in o-ring seal conjunctions with hydraulic fluids. Stupkiewicz and Marciniszyn [22] considered a hyperelastic (Mooney–Rivlin) FEA model to represent the seal deformation behaviour under load. They showed that a coherent film of lubricant is only present when fully developed elastohydrodynamic regime of lubrication is encountered. The soft mixed-elastohydrodynamic approach has also been applied to alternative sealing geometries, such as rotary lip seals [23], while Ruskell [24] showed that rectangular seals form appreciably thinner films than the o-rings.

A thin lubricant film thickness is one of the problems with elastomeric seals in drug delivery devices, including inhalers. The behaviour of reciprocating seals with rectangular cross sections, typical of seals in some drug delivery devices, has also been studied in hydraulic actuators under relatively high loads [25,26]. The authors considered the elastic deformation of the seal due to global fitment deformation under a differential applied pressure. It was found that for strains below 10%, the classical linear elasticity theory suffices. Viscous friction due to the shear of a lubricant film was calculated. It was shown that operating speeds greatly influence the lubricant film thickness as does edge profiling of the seal contact geometry. They suggested that an optimum operating speed exists in terms of film thickness and leakage, as does an optimum seal interference fit value. However, there is still a dearth of knowledge regarding the frictional and sealing characteristics of elastomeric o-ring seals under quite low loads, particularly with drug formulations which lack a sufficient degree of lubricity. This is a

poignant problem as the propellant, constituting 99% of most formulations [3] also effectively acts as the bio-compatible lubricant, with very poor viscosity in the range 0.15–0.5 mPa s (over a temperature range of −50° C to +60° C).

The aim of this work is to investigate the contact behaviour of typical *pharmaceutical seals*, such as those met in pMDIs. The effect that the deformation of elastomeric seals has on the lubrication of medical devices is of particular interest. A methodology for the calculation of the seals' *in situ* deflection is proposed, taking into account their global and local distortions, which are then used to solve Reynolds equation. The numerical method allows prediction of contact pressure distribution and, thus, the lubricant film thickness variation along the seal face-width. This is a radically different approach compared with the empirical equations that are generally employed in such investigations [14,15]. An extrapolated equation is derived as a by-product of the current analysis, in order to accelerate the simulation time within prescribed range of values of the main parameters (speed of entraining motion and contact load), when used in industrial environments. The developed extrapolated equation is the first reported for study of lubrication of medical devices, employing elastomeric contacting elements. The main assumptions behind the current analysis are presented, as well as suggestions for future investigations.

2. Mathematical model

2.1. Lubricant film shape

There are various inhaler valve configurations. In the particular type under investigation here, elastomeric seals are fitted to the actuating stem and move in concert with it (see Fig. 1(a)). This assembly is fitted into the housing bore as shown in Fig. 1(b), confining the formulation within the canister. The deformed shape of the seal is as the result of fitment stresses and the applied canister pressure. Fig. 1 shows the undeformed and deformed (*in situ*) cross-sectional shapes of an inhaler valve seal. It is important to determine the *in situ* profile of the seal in contact with the actuating stem and the housing bore in order to predict the prevailing contact conditions. The cross section of the seal under investigation is assumed to be in contact with both the stem and the housing bore (Fig. 1) during the seal fitment within its retaining groove. There are effectively three stages in the fitment process. These are changes in seal's nominal diameter, application of differential canister pressure and cross-sectional shape changes to conform to the groove geometry. During the process the seal is assumed to be constrained by the groove boundaries (stem and housing).

A thin film of lubricant, carrying the contact load, is formed between the stem and the seal due to the limited access of the entrained fluid to seal-housing bore conjunction. The thickness of any film of fluid which may be entrained into the conjunction between the seal and the housing is mainly as the result of seal deflection from its original undeformed state to its *in situ* shape. Therefore, the size and shape of the film layer depends on the global *in situ* deformation of the elastomeric seal (this is regarded as an "elastic" film shape). There are two phenomena giving rise to seal deflection. One is its global deflection, with relatively large strains during fitment and also due to pressure gradient across it. The other is the local small strain deflection

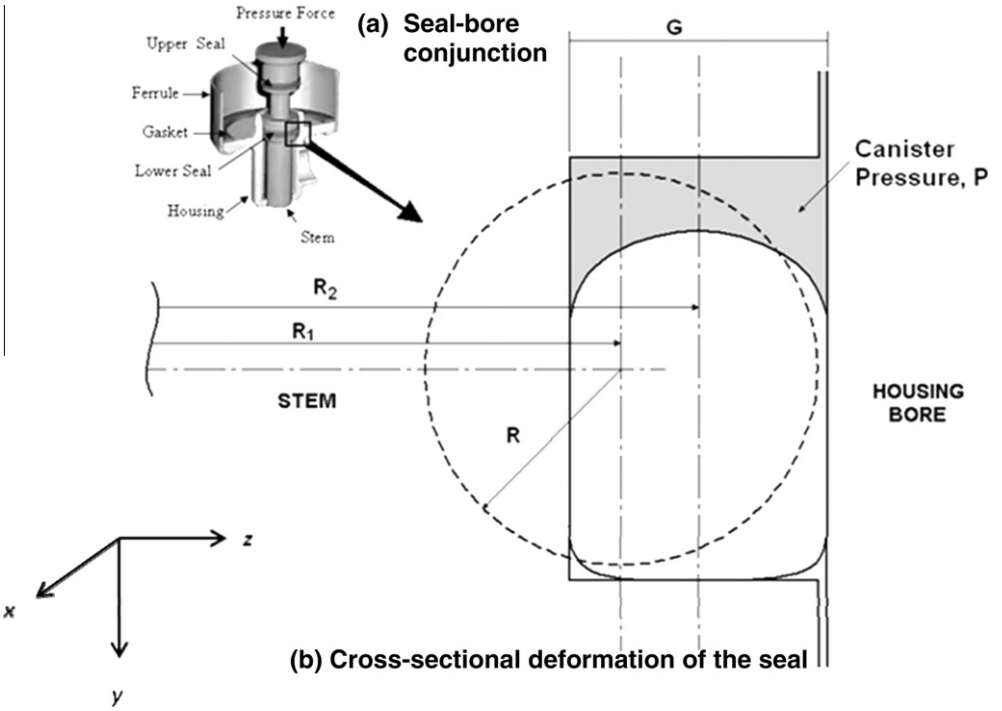

Fig. 1. Fitted geometry of the valve seal.

which may be caused as the result of the generated conjunctional pressures. As stated above, the contact between the o-ring seal and its rectangular groove may be regarded as a one-dimensional lubricated conjunction in the first instance. The "elastic" film shape is given as:

$$h(y) = h_0 + S(y) + \delta(y) + \Delta(y), \tag{1}$$

$S(y)$ is the initial undeformed profile of the o-ring seal along its face-width y, assumed to be parabolic: $S(y) = \frac{y^2}{2R_{zy}}$ and for a rectangular groove the equivalent radius $R_{zy} = R$. h_0 is any initial gap which may exist after fitment and applied canister pressure. Therefore, the term $S(y) + \Delta(y)$ is the deformed seal *in situ* shape, where $\Delta(y)$ is the global deflection imposed during seal fitment in the groove and as the result of canister pressure. This is the global compressive deflection, which was originally defined by Lindley [7]. $\delta(y)$ is the localised contact deflection along the y direction due to the generated pressures in the seal-stem conjunction. Note that in this preliminary analysis a one dimensional solution of the Reynolds equation is assumed in the direction of sliding, y (seal deformed face-width).

2.2. Determination of global deflection

The global deflection of the seal $\Delta(y)$ caused during its fitment in its retaining groove (Fig. 1) is calculated using a method developed by Muskhelishvili [4]. The seal is in contact with both stem and the housing along the direction y. The calculation of elastic equilibrium of a circular disk (undertaking purely plane deformations) under known external forces acting on its boundaries, has been used in the current analysis for the two of the three stages of the seal's fitment process; application of the differential canister pressure and any change in the seal cross sectional shape, so that it would conform to its retaining groove. Here the assumed undeformed circular cross-section of the o-ring is considered as a disc. Flamant [27] provided the original solution for a circular disk subjected to a concentrated force acting upon its boundary.

When two equal and opposite forces P (per unit computation element width) act at points Z_1 and Z_2, parallel to the Oz axis as shown in Fig. 2, then Muskhelishvili [4] showed that the principle of superposition may be used to determine the induced stresses at any point Z within the disc as:

$$\begin{aligned}
\sigma_z &= \frac{2P}{\pi}\left(\frac{\cos^3 a_1}{r_1} + \frac{\cos^3 a_2}{r_2}\right) - \frac{P}{\pi R}\cos b,\\
\sigma_y &= \frac{2P}{\pi}\left(\frac{\sin^2 a_1 \cdot \cos a_1}{r_1} + \frac{\sin^2 a_2 \cdot \cos a_2}{r_2}\right) - \frac{P}{\pi R}\cos b,\\
\tau_{zy} &= -\frac{2P}{\pi}\left(\frac{\sin a_1 \cdot \cos^2 a_1}{r_1} - \frac{\sin a_2 \cdot \cos^2 a_2}{r_2}\right).
\end{aligned} \tag{2}$$

The cross-section of the o-ring seal is assumed to be a circular disc subjected to distributed external unit loads, P. The stress at any point Z of the disk is then obtained as the cumulative result of all such equal and opposite force pairs applied at regular boundary nodes, in accordance with Eq. (2). Thus, the overall stress components at any cross-sectional location Z are obtained according to a pre-determined grid domain. The discretisation of the seal's cross section is made at 1° intervals (giving a total of 16021 nodes). Fig. 3 shows a 90° segment of the seal's discretised cross-section.

Thus, in accordance with the assumed plane strain conditions:

$$\begin{aligned}
\varepsilon_{zi} &= \frac{1-\upsilon^2}{E}\sigma_{zi} - \frac{\upsilon(1+\upsilon)}{E}\sigma_{yi},\\
\varepsilon_{yi} &= \frac{1-\upsilon^2}{E}\sigma_{yi} - \frac{\upsilon(1+\upsilon)}{E}\sigma_{zi},\\
\gamma_{zyi} &= \frac{2(1+\upsilon)}{E}\tau_{zyi},
\end{aligned} \tag{3}$$

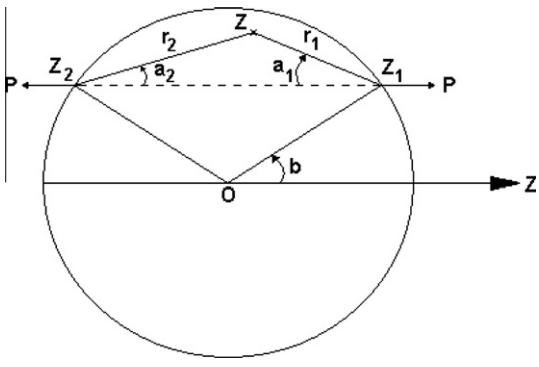

Fig. 2. A pair of concentrated forces acting on a circular disc.

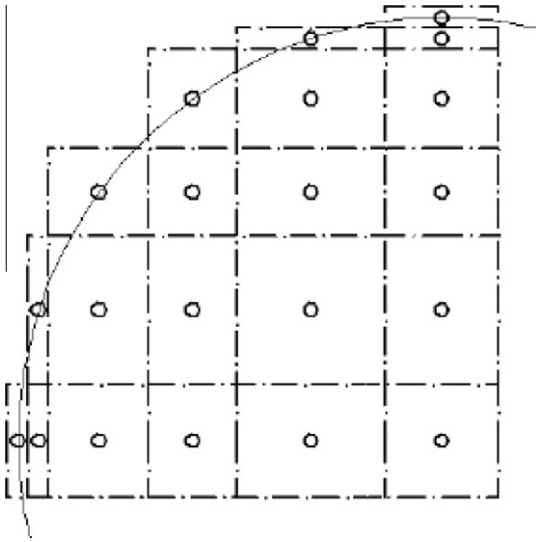

Fig. 3. A 90° segment of the seal's discretised cross section.

where

$$\sigma_{zi} = \frac{P}{\pi}\sum_j \left\{ 2\left(\frac{\cos^3 a_{1ij}}{r_{1ij}} + \frac{\cos^3 a_{2ij}}{r_{2ij}} \right) - \frac{\cos b_j}{R} \right\},$$
$$\sigma_{yi} = \frac{P}{\pi}\sum_j \left\{ 2\left(\frac{\sin^2 a_{1ij} \cdot \cos a_{1ij}}{r_{1ij}} + \frac{\sin^2 a_{2ij} \cdot \cos a_{2ij}}{r_{2ij}} \right) - \frac{\cos b_j}{R} \right\}, \tag{4}$$
$$\tau_{zyi} = -\frac{2P}{\pi}\sum_j \left\{ \frac{\sin a_{1ij} \cdot \cos^2 a_{1ij}}{r_{1ij}} - \frac{\sin a_{2ij} \cdot \cos^2 a_{2ij}}{r_{2ij}} \right\},$$

i denotes a point such as Z within the seal cross-section, whilst j refers to a pair of conjugate seal boundary nodes, parallel to the axis oz in Fig. 2 (chords through the cross section such as Z_1Z_2). The terms in the summation represent the influence coefficients. If non-uniform regional loading is to be considered, such as that proposed by Green and English [10,11], then (P is replaced by P_j and becomes a part of the summation process. Thus, along any chordal distance, such as Z_1Z_2 (see Fig. 2), the global deflection of the seal's cross section is the cumulative sum:

$$\Delta(y) = \sum_i \sum_j L_{yj}\varepsilon_{zi}, \tag{5}$$

L_{yi} is the length of a domain element under consideration, while ε_{zi} denotes its particular strain. The above method is followed for two of the stages of the seal's fitment in the groove; the influence coefficients are combined with the corresponding loads on the seal's boundaries in each stage of analysis. The superposition of these steps (additionally to the change in seal's nominal diameter) leads to the calculation of the total amount of global deflection $\Delta(y)$ that contributes to the "elastic" film shape equation.

2.3. Determination of local deflection

The localised deflection $\delta(y)$ at any contact location along the y direction in Eq. (1) is due to the generated pressures in the seal-canister wall (bore) conjunction. This is obtained as:

$$\delta(y) = -\frac{2}{\pi E'}\int_{y_i}^{y_e} p(y)\ln(y-y')^2 dy', \tag{6}$$

where the limits of the integral represent the extent of conjunctional pressure distribution from the inlet to its outlet; the film rupture position y_e, determined by the Swift–Stieber boundary condition. Eq. (6) is put in non-dimensional form as:

$$\overline{\delta} = -\frac{1}{2\pi}\left[\int_{Y_i}^{Y_e} p^* \ln\left(Y-Y'\right)^2 dY' + \ln\left(\frac{8W^*R^2}{\pi}\right)\int_{Y_i}^{Y_e} p^* dY' \right], \tag{7}$$

where

$$\begin{aligned} y &= bY, \\ p &= p_H p^*, \\ \delta &= \frac{b^2\bar{\delta}}{R}, \\ W^* &= \frac{w}{E'Rl}, \\ \frac{1}{E'} &= \frac{1}{\frac{1-v^2}{E}+\frac{1-v_p^2}{E_p}}. \end{aligned} \tag{8}$$

The normal load per unit width can be found by integrating the pressure from inlet to outlet, thus:

$$w = \int_{y_i}^{y_e} p dy', \quad \text{hence}: \int_{Y_i}^{Y_e} p^* dY' = \frac{\pi}{2}. \tag{9}$$

Substituting back into Eq. (7) and carrying out the integration yields:

$$\bar{\delta} = -\frac{1}{2\pi}|p^* I|_{Y_i}^{Y_e} + \frac{1}{2\pi}\int_{Y_i}^{Y_e} \frac{dp^*}{dy'} I dY' - \frac{1}{4}\ln\left(\frac{8W^*R^2}{\pi}\right), \tag{10}$$

where

$$I = \int (Y-Y')^2 dY' = -(Y-Y')\left[\ln(Y-Y')^2 - 2\right]. \tag{11}$$

Assuming that $p^* = 0$ at Y_i and Y_e, Eq. (10) can be discretised for a grid of n computation points, which for a bounded ring becomes:

$$\bar{\delta}_i = \sum_{k=1}^{n} D_{i,k} p_k^*, \tag{12}$$

where k represent a pressure node, whilst i represents a point where a localised surface deflection is evaluated. $D_{i,k}$ are the influence coefficients which are calculated, following the method described in Section 2.2. The non-dimensional form of the elastic film shape, using the dimensionless groups in (8) becomes:

$$H(Y) = H_0 + \frac{Y^2}{R} + \bar{\delta} + \bar{\Delta}, \tag{13}$$

where the film thickness h and global fitment deformation Δ are normalised in the same manner as δ.

2.4. Reynolds' equation

The "elastic" film shape Eq. (1) has to be solved simultaneously with Reynolds' equation to obtain the corresponding conjunctional pressures. As an initial solution a long line contact approach is assumed. This means that the seal-stem conjunction is that along the seal face-width. Thus, the simplified form of Reynolds' equation is:

$$\frac{d}{dy}\left(\frac{\rho h^3}{\eta}\frac{dp}{dy}\right) = 12u\frac{d(\rho h)}{dy}, \tag{14}$$

where $u = (u_1 + u_2)/2$ is the speed of entraining motion of the fluid into the conjunction. This is effectively half the actuation speed of the device (sliding speed of the stem).

With fairly uniform actuation speed, the effect of squeeze film action is ignored. Furthermore, no side leakage in the circumferential direction, x (see Fig. 1) is expected.

Now using the same non-dimensional parameters as in Eq. (8) and $\bar{\rho} = \rho/\rho_0$, $\bar{\eta} = \eta/\eta_0 = e^{\alpha p}$:

$$\frac{d}{dY}\left(\frac{\bar{\rho}H^3}{\bar{\eta}}\frac{dp^*}{dY}\right) = 24U^*\sqrt{\frac{2W^*}{\pi}}\frac{d(\bar{\rho}H)}{dY}, \tag{15}$$

where $U^* = u\eta_0/E'R$.

The formulation is considered to act as an iso-viscous fluid with no density variation, thus one can ignore $\bar{\rho}$ in Eq. (15) and let $\bar{\eta} = 1$. As already described, Swift–Stieber exit boundary conditions are employed to solve Reynolds' equation:

$$p^* = p_e^* = 0, \quad \frac{\partial p^*}{\partial Y} = 0 \text{ at } Y = Y_e. \tag{16}$$

The inlet boundary condition is given as:

$$p^* = p_c^* \text{ at } Y = Y_i = \frac{1}{2}b. \tag{17}$$

3. Method of solution

There are two stages in the solution procedure. First, the *in situ* globally deformed shape of the seal is determined through the dry elastostatic analysis of seal fitment with the following steps:

Step 1: Calculation of the tension of the seal's cross section, as this is stretched from its original (manufactured) position to the centre of the groove (because of a difference between the stem diameter and the original internal diameter of the seal). The centreline of the seal moves from R_1 to R_2 in Fig. 1. This action is physical placement of the undeformed circular cross section of the seal to the groove centre. The circumferential length of the undeformed seal's centreline is then calculated as well as that of the groove's centreline. From these two values, the elongation required (difference between unloaded seal and the centreline of the groove) is determined. The latter is used to find the strain produced as the result of elongation:

$$\varepsilon_x = \Delta\ell/2\pi R_1, \quad \text{where} \quad \Delta\ell = 2\pi(R_2 - R_1).$$

Therefore, the stress is calculated (E is Young's modulus of the seal's elastomer) as:

$$\sigma_x = E \cdot \varepsilon_x.$$

Then, the strain is calculated for every element of the cross section (ν is Poisson's ratio of the seal's elastomer):

$$\varepsilon_y = -(\nu \cdot \sigma_x)/E \quad \text{and} \quad \varepsilon_x = -(\nu \cdot \sigma_x)/E.$$

Therefore, the deflection of every element can be calculated, using Eq. (5). This is the first term of global deflection $\Delta_1(y)$.

Step 2: This causes the deformation of the seal's cross section, because of the canister pressure applied on its boundary. The method described in Section 2.2 is now applied to determine the second term of global deflection $\Delta_2(y)$.

Step 3: Finally, the global deflection of the seal's cross section is calculated due to fitment in the groove as: $\Delta_f = D - G$, where G is the groove width (Fig. 1). Therefore, the radial strain through its cross-section is: $\varepsilon_z = \frac{\Delta_f}{D}$. Again, the methodology described in Section 2.2 is applied to calculate the deflection for each element of the cross section, using an iterative process. This is the third term of global deflection $\Delta_3(y)$.

Step 4: Assuming the elastomeric seal to be an incompressible elastic solid, then the dilatation $\nabla = 0$. Hence, $\varepsilon_y = -\varepsilon_z$ and the effective contact face-width for seal-groove conformance is determined as: $b = c(1 + \varepsilon_y)$ (note that the seal face-width changes during fitment).

Step 5: Initially, a Hertzian elastic line contact may be assumed, thus the load per unit length of the seal is obtained as $P = \frac{w}{l} = \frac{\pi E' c^2}{4R}$. This is an initial uniform elastic line contact Hertzian pressure distribution across the seal face-width, with no edge stress discontinuity [28]. This initial guess for load per unit length is then applied on the elements covering the calculated effective face-width, resulting in the corresponding boundary load values of step 3 (third term of global deflection $\Delta(y)$). Subsequent iterations use the following procedure and clearly deviate from the Hertzian conditions.

Step 6: Stresses and strains are now obtained using the method highlighted in Section 2.2, finally yielding the actual fitment deflection $\Delta_3(y)$.

Step 7: The following convergence criterion is used:

$$\frac{\Delta_f - \Delta_3(y)}{\Delta_3(y)} \leqslant \varepsilon_f. \tag{18}$$

Step 8: The fitment load per unit length is increased, if convergence is not achieved:

$$P^k = P^{k-1} + \frac{\beta}{n}\left(\frac{\Delta_f - \Delta_3(y)}{\Delta_3(y)}\right), \tag{19}$$

where n is the number of elements used to discretise the effective face-width b. The procedure is then repeated until the convergence criterion (18) is satisfied. Clearly, the pressure distribution (thus load per unit width of contact) alters significantly from the initial Hertzian assumption.

The second stage of the analysis concerns soft elastohydrodynamics of seal-groove conjunction in relative motion. The procedure is the combined solution of Reynolds Eq. (15), the elastic film shape (13) with Eq. (12) in an iterative procedure involving low relaxation effective influence Newton–Raphson method with Gauss–Seidel iterations as described in detail by Jalali-Vahid et al. [29]. Two convergence criteria should be satisfied, as described below.

Step 9: First a pressure convergence criterion is sought where:

$$\sum_{k=1}^{n}\left|\frac{p_k^{*j} - p_k^{*j-1}}{p_k^{*j}}\right| \leqslant \varepsilon_{p^*}, \tag{20}$$

when this condition is not met, the pressures are adjusted using under-relaxation as:

$$p_k^{*j} = p_k^{*j-1} + \chi \Delta p_k^{*j}, \tag{21}$$

where j is an iteration counter, $0 < \chi < 1$ is an under-relaxation factor and Δp_k^{*j} are the pressure differences in each iterative step j.

Step 10: Contact pressure values p_k^* obtained at any nodal position k within the effective contact face-width b, which are found to be sub-ambient, are discarded. Then, the contact load is obtained as the integrated pressure distribution (lubricant reaction) as: $\overline{W} = dY \sum_{k=1}^{n} p_k^*$, dY being the computational element size; $dY = b/n$.

Step 11: The calculated lubricant reaction must satisfy the following load convergence criterion (see Eq. (9)):

$$\overline{W} - \frac{\pi}{2} \leqslant \varepsilon_{\overline{W}}. \tag{22}$$

If this criterion is not met, the small assumed gap size is altered as:

$$H_0^j = H_0^j - \zeta \left| \overline{W} - \frac{\pi}{2} \right|, \tag{23}$$

and steps 9 through 11 are repeated.

4. Results and discussion

The seal under examination is of circular shape with a circular cross section. Information concerning material properties and seal geometry is provided in Table 1.

A series of simulations were carried out with HFA 134A as the propellant, in some cases with a siliconised seal. The dynamic viscosity of HFA under the simulated conditions is 0.21 mPa s, whilst that of silicone oil is 0.91 mPa s. The contact pressure distribution is significantly affected by the canister pressure. Fig. 4 shows a series of contact pressure distributions with HFA as the lubricant for an *in situ* seal subjected to different canister pressures. Poor viscosity of HFA means that these pressures may be regarded as dry elastostatic. It is noteworthy that the overall shape of the distribution only resembles a Hertzian pressure profile, but in fact they significantly differ from it. Thus, the assumption of an elliptical Hertzian pressure profile made by Karaszkiewicz [13–15] is not appropriate. The maximum Hertzian pressure for the canister pressure of 0.29 MPa would be 0.62 MPa, instead of the actual value of 0.94 MPa as shown in Fig. 4, an error of 34%. The seal face-width after fitment is that shown for the case with no canister pressure (the case of a dry inhaler valve). This is around 0.7 mm. It increases with canister pressure as shown in the figure. The contact load reaches a value of 12.4N (as a result of the integrated pressure) when the canister pressure is 0.55 MPa.

As shown in Fig. 4, the pressure at the ends of the contact zone diminishes (i.e. not equalling the canister pressure). This is due to the way in which the canister pressure is taken into account in the numerical model. The effect of the canister pressure has already been considered, when calculating the global deflection, through the term $\Delta_2(y)$. The latter is used in the formation of the film shape function when solving Reynolds' equation, as the physical contribution of the canister pressure on the film shape.

Additionally, no element reaches strains above 6%, while the maximum fractional compressions are in the region of 15%. The ratio of the seal's cross-section over the contact width is approximately 2. The above values are within the limits which permit the use of linear elasticity as shown by Nikas and Sayles [25] and Kim et al. [12].

The valve actuation speed of 0.03 m/s (a test speed often used for inhalation devices) is insufficient to promote entrainment of a film of fluid into the conjunction, particularly for the propellants/lubricants used. The pressure profile for the siliconised seal almost coincides with that for the case of HFA for the canister pressure of 0.55 MPa in Fig. 4. There are clearly some subtle differences; a slightly longer inlet trail and very slightly shorter exit region, both of which are difficult to discern in the chosen scale of Fig. 4. The differences are best noted in the film thickness profiles in Fig. 5. A film of silicone oil is assumed to form on the seal's face-width with any shearing action. Clearly, with a higher dynamic viscosity the film of silicone oil has a higher load carrying capacity. Thus, at the same contact load of 12.4N, determined by the fitment stresses and the applied canister pressure, the silicone oil forms a thicker film than the HFA. However, in both cases the predicted film is of

Table 1
Material properties and characteristic dimensions.

Parameter	Value
Undeformed cross sectional seal diameter	1.61 mm
Outer seal diameter	6 mm
Seal groove width G	1.36 mm
Elastic modulus of the stem (E_p)	2.6 GPa
Elastic modulus of the seal (E)	2.5 MPa
Poisson's ratio of the stem (ν_p)	0.35
Poisson's ratio of the seal (ν)	0.49

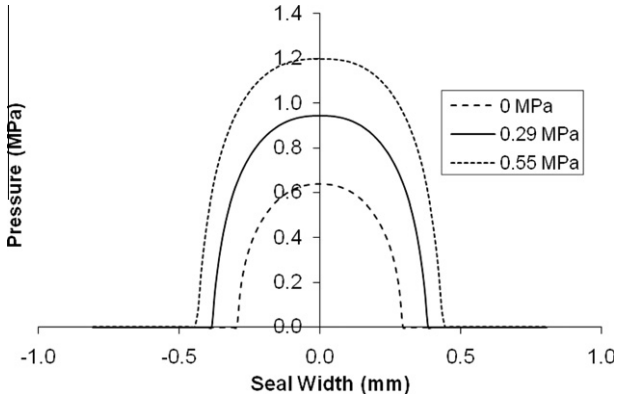

Fig. 4. Seal contact pressure distributions at different canister pressures.

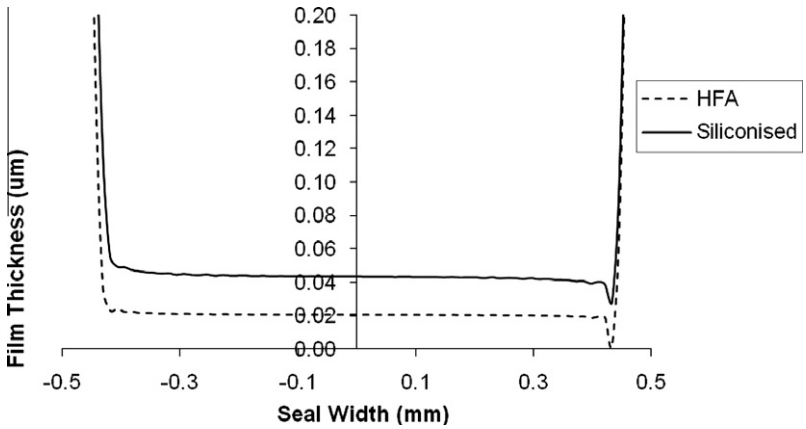

Fig. 5. Film thickness in the rubber seal conjunction.

insufficient thickness to guard against boundary interaction of surfaces. The film thickness shape clearly indicates the prevalent elastohydrodynamic regime of lubrication (EHL), but with hardly any piezo-viscous action of the lubricant in both cases. This form of EHL is often termed as an iso-viscous elastic regime of lubrication or soft EHL.

An important observation is that the predicted film thickness is significantly thinner than the root mean square roughness (RMS) of the usual counterfaces. Typical values of the counterface RMS roughness are 0.5–1 μm. Therefore, the very thin film combined with the measured characteristics of the surface roughness between the seal and housing indicate boundary or at best mixed regime of lubrication. These findings conform well with in-field observations and experimental tests reported by Grimble et al. [2], where surface roughness was taken into consideration. They are also in accord with the findings of Stupkiewicz and Marciniszyn [22] that a coherent film is not formed unless elastohydrodynamic conditions are fully developed.

There is no definitive evidence to suggest that siliconised rubber seal surfaces are sustained after repeated use of the pMDIs. It is important to note that the boundary nature of regime of lubrication is often the reason for the use of silicone oil (polydimethylsiloxane) on the elastomeric seals. In fact silicone oil is used as a boundary lubricant, because the methyl functional groups form bonding of cation to rough surfaces fairly uniformly. However, with poor lubrication of seals, presence of silicone oil makes only marginal improvement as already shown. Therefore, it is safe to assume that HFA would remain the main source of elastomeric seal lubricity. It is also clear that the low actuation test speed, commonly adopted may be exceeded significantly by the users of pMDIs. Since the speed of entraining motion (half the sliding speed of the stem in this case) is the main contributory factor in film formation under EHL, then there is the chance of thicker films with higher actuation speeds. The effect of increasing the sliding speed upon film thickness is shown in Fig. 6.

Although a thicker film is predicted by increasing the actuation speed by more than an order of magnitude, it is clear that a fully fluid film regime of lubrication cannot be attained. Another observation from Figs. 5 and 6 is that the film thickness follows small oscillations (ripples) along the seal face-width. These occur as the result of convergence issues of the numerical method for the boundary nodes of the cross section during the seal fitment to its retaining groove process. Initially, the discretisation of the seal's cross section was made at 1° intervals (Fig. 3). Every effort was made to ensure that a node lies on the boundary, while a tight convergence criterion was employed in the numerical analysis. However, there was small variation

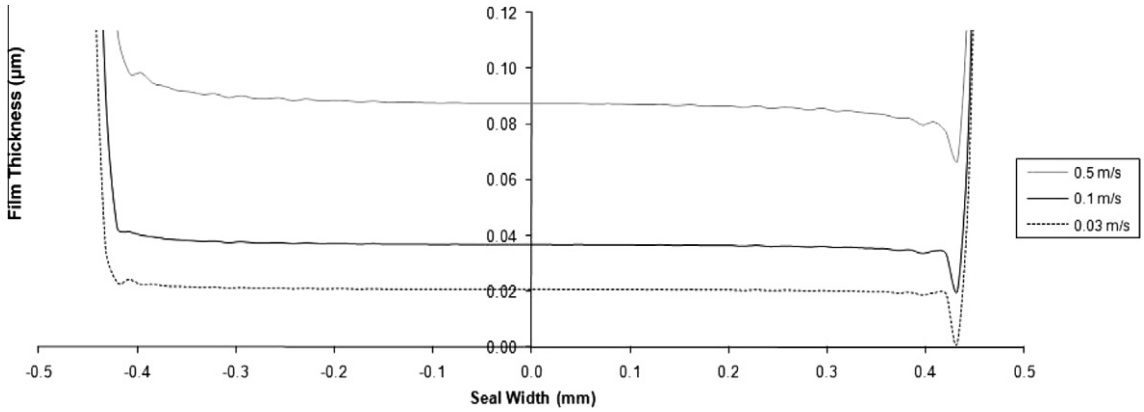

Fig. 6. Film thickness variation with increasing actuation (sliding) speed.

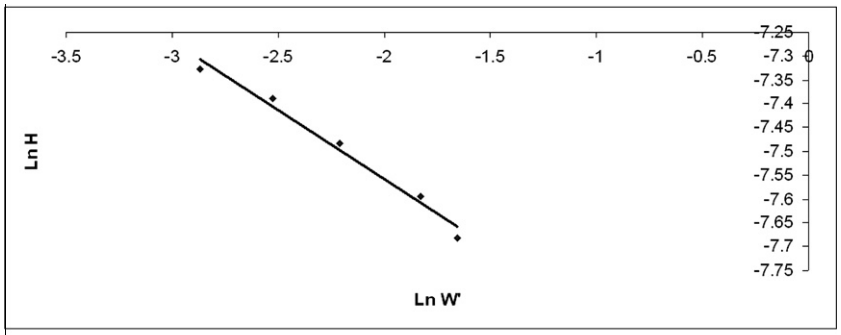

(a) **Variation with load parameter**

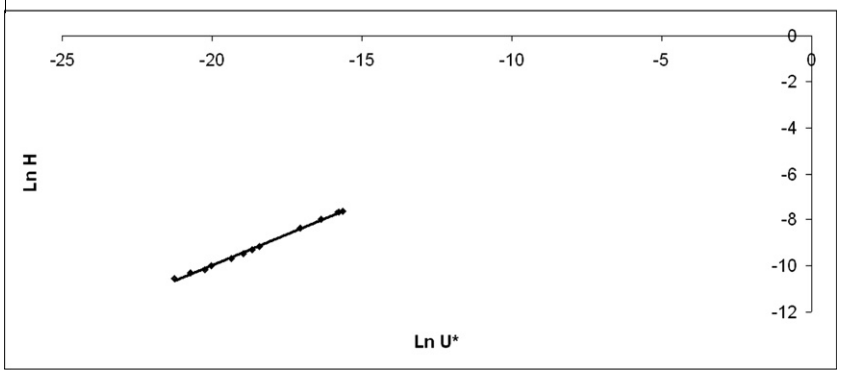

(b) **Variation with speed parameter**

Fig. 7. Film thickness variation with the governing parameters.

from node to node, especially since adjusting a boundary load pair influences each and every surrounding element/node. A denser discretisation was carried out at 0.5° intervals. While the convergence time was dramatically increased, the results showed little improvement in terms of the aforementioned ripples. However, in general the simulation times are quite long, given the computational procedure described in Section 3. It is usual to obtain extrapolated oil film thickness equations by regression of numerical results. This paves the way for estimation of film thickness, thus regime of lubrication and friction, sympathetic to the prevalent short time-scales in industrial environments.

Simulations were carried out for a range of values of U^* and W^*. The range of values were chosen to represent contact loads arising from typical piece-to-piece variations in the seal dimensions, changes in canister pressure during the pMDI valve actuation or seal swelling because of ingestion of formulation owing to the structural porosity of elastomers. Although

the standard valve compression tests in industry are at the low actuation speed of 0.03 m/s, its in-field use is often subject to much higher stem sliding speeds as shown, for example, in Fig. 6. The range of values used for the extrapolated lubricant film thickness equation was: $0.0566 \leqslant W^* \leqslant 0.19055$ and $9.87 \times 10^{-10} \leqslant U^* \leqslant 1.58 \times 10^{-7}$ with 20 simulation runs.

Fig. 7(a) and (b) show logarithmic variations of the dimensionless film H with the governing parameters W^* and U^*, yielding the extrapolated equation found through regression analysis as:

$$H = 1.49 U^{*^{0.54}} W^{*^{-0.29}}. \tag{24}$$

Karaszkiewicz [14,15], as well as Grimble et al. [2] used Hamrock and Dowson [16] equation for an EHL line contact of materials of low moduli:

$$H = 4.4 U^{*^{0.65}} W^{*^{-0.21}}. \tag{25}$$

Note that Eq. (25) is based on an implied counterformal line contact with Hertzian contact condition. Both equations show a greater sensitivity to load than is the case for hard EHL conditions with materials of high elastic modulus. This is because the regime of lubrication is in fact iso-viscous elastic. Fig. 8 shows the predicted conditions plotted in the Greenwood Chart [30]. The abscissa in this figure is termed the elastic parameter G_e, whilst the ordinate is defined as the viscous parameter G_v:

$$G_e = \frac{W^{*^{8/3}}}{U^{*^2}} \quad \text{and} \quad G_v = \frac{G^* W^{*^3}}{U^{*^2}}, \tag{26}$$

where the materials' parameter is: $G^* = E'\alpha$.

The power exponent of the speed parameter is in line with the dominance of speed of entraining motion in formation of EHL films. Gohar and Rahnejat [28] show that this exponent is in the range 0.68–0.7 for hard EHL conjunctions, which is slightly reduced to 0.65 [16] under iso-viscous elastic conditions. Again, because of deviation from Hertzian conditions and greater degree of conformity of seal to its retaining groove, the inlet wedge effect is reduced, resulting in lesser sensitivity to speed of entraining motion. Therefore, the more detailed analysis here compared with the empirical approach highlighted by Karaszkiewicz [14,15] indicates thinner predicted lubricant films under the same operating conditions. This is shown in Fig. 9(a) and (b) as functions of the operating parameters. The solid line in both cases represents the results obtained through use of the new extrapolated equation.

5. Concluding remarks and future work

The analysis carried out corroborates the assumption made based on the predominance of boundary regime of lubrication, as noted by Grimble et al. [2] and Prokopovich et al. [18]. The predicted lubricant film in both examined cases (HFA and silicone oil) is of insufficient thickness to guard against boundary interaction of surfaces. The film thickness shape clearly indicates the prevalent elastohydrodynamic regime of lubrication (EHL) while the contact pressure distribution significantly differs from a Hertzian pressure profile. The latter, as well as the greater degree of seal conformity to its retaining groove, are the main reasons behind the reduced sensitivity of the derived extrapolated equation to the speed of entraining motion.

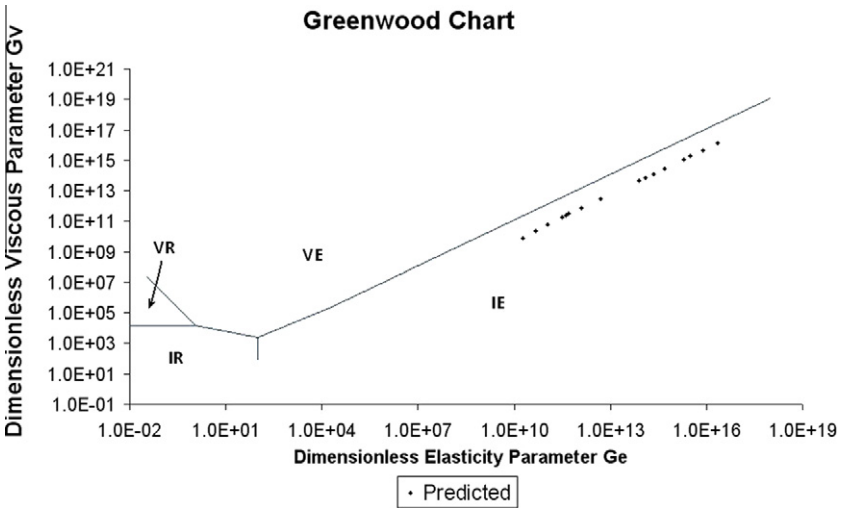

Fig. 8. Prevailing regime of lubrication in the inhaler valve seal conjunction. *Key*: IR, iso-viscous rigid; IE, iso-viscous elastic (*soft EHL*); VR, viscous rigid; VE, viscous elastic (*hard EHL*).

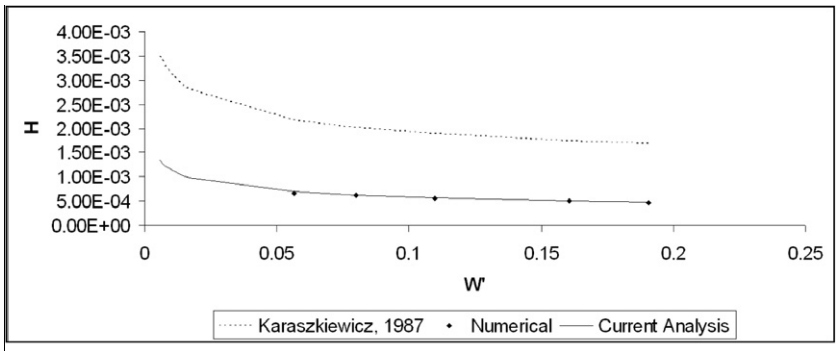

(a)- Variation with load parameter

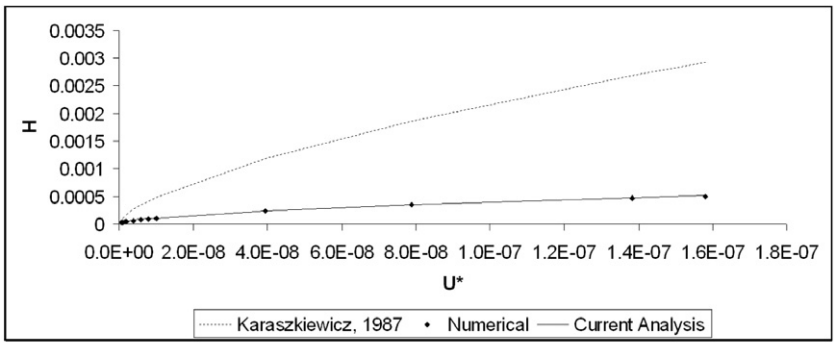

(b)- Variation with speed parameter

Fig. 9. Film thickness variation with governing operational parameters.

Therefore, the work presented indicates thinner predicted lubricant films compared with the empirical approach highlighted by Karaszkiewicz [14,15] under the same operating conditions.

The current analysis, although detailed, embodies a certain number of assumptions including iso-viscous action of the fluid. Whilst this is justified for the rather non-reactive HFA propellant, the same cannot be taken for granted in the case of siliconised rubber seal surfaces. Silicone oil is quite sensitive to shear rate, acting rather like a gel; in solid state at low shear and as liquid lubricant while the shear rate is increased [31]. Therefore, further work is required to ascertain the real effect of siliconisation of valve seals. Furthermore, the chamber temperature alters, thus that of the formulation during the atomisation process. The viscosity of the fluid may increase sufficiently to increase its load carrying capacity, thus enhance the lubricant film thickness. This calls for a thermal balance equation to be integrated with the current analysis. However, a suitable thermo-viscous model for such complex formulations is not currently available. Finally, the inclusion of surface roughness would be another key aspect for future work, where the effect of adhesion between the interacting surfaces may be examined.

Acknowledgements

The authors would like to express their gratitude to the Engineering and Physical Sciences Research Council (EPSRC) for sponsorship of this research as well as 3M Health Care Ltd. for both financial and technical support.

References

[1] T.S. Purewal, D.J.W. Grant, Metered Dose Inhaler Technology, Taylor and Francis, London, 1978.
[2] D.W. Grimble, S. Theodossiades, H. Rahnejat, M. Wilby, Tribology of rough ultra-film contacts in drug delivery devices, Proc. Inst. Mech. Eng. C. J. Mech. Eng. Sci. 222 (2008) 2209–2216.
[3] T. Noakes, Medical aerosol propellants, J. Fluorine Chem. 118 (2002) 35–45.
[4] N.I. Muskhelishvili, Some Basic Problems of the Mathematical Theory of Elasticity: Fundamental Equations, Plane Theory of Elasticity, Torsion and Bending, second ed., Noordhoff, Groningen, 1953.
[5] J.H. Michell, Elementary distributions of plane stress, Proc. Lond. Math. Soc. 32 (1901) 35–61.
[6] A.E.H. Love, A Treatise on the Mathematical Theory of Elasticity, fourth ed., Cambridge University Press, Cambridge, 1927.
[7] P.B. Lindley, Compression characteristics of laterally-unrestrained rubber O-rings, J. Inst. Rubber Ind. (July/August) (1967).
[8] A.F. George, A. Strozzi, A.J. Rich, Stress fields in a compressed unconstrained elastomer o-ring seal and a comparison of computer predictions and experimental results, Tribol. Int. 20 (1987) 237–247.

[9] E. Dragoni, A. Strozzi, Analysis of an unpressurised, laterally restrained, elastomeric o-ring seal, J. Tribol. Trans. ASME 110 (1988) 193–200.
[10] I. Green, C. English, Analysis of elastomeric o-ring seals in compression using the finite element method, Tribol. Trans. 35 (1992) 83–88.
[11] I. Green, C. English, Stresses and deformation of compressed elastomeric o-ring seals, in: 14th International Conference on Fluid Sealing, 6–8th April, BHR Group Cranfield, 1994.
[12] H. Kim, S. Park, H. Lee, D. Kim, Y. Lee, Approximation of contact stress for a compressed and laterally one side restrained O-ring, Eng. Fail. Anal. 14 (2007) 1680–1692.
[13] A. Karaszkiewicz, Hydrodynamic lubrication of rubber seals for reciprocating motion: leakage of seals with an o-ring, Tribol. Int. 21 (1985).
[14] A. Karaszkiewicz, Hydrodynamics of rubber seals for reciprocating motion, lubricating film thickness, and out-leakage of O-seals, Ind. Eng. Chem. Res. 26 (1987).
[15] A. Karaszkiewicz, Geometry and contact pressure of an O-ring mounted in a seal groove, Ind. Eng. Chem. Res. 29 (1990) 2134–2137.
[16] B.J. Hamrock, D. Dowson, Elastohydrodynamic lubrication of elliptical contacts for materials of low elastic modulus I. Fully flooded conjunction, J. Lubric. Technol. Trans. ASME 100 (1978) 236–245.
[17] J.A. Greenwood, J.H. Tripp, The contact of two nominally flat rough surfaces, Proc. Inst. Mech. Eng. J. Mech. Eng. Sci. 185 (1971) 625–633.
[18] P. Prokopovich, S. Theodossiades, H. Rahnejat, D. Hodson, Friction in ultra-thin conjunction of valve seals of pressurised metered dose inhalers, Wear 268 (2009) 845–852.
[19] C.J. Hooke, D.J. Lines, J.P. O'Donoghue, Elastohydrodynamic lubrication of O-ring seals, Proc. Inst. Mech. Eng. 181 (Pt 1) (1966–1967) 205–210.
[20] L.M. Milne-Thomson, Plane Elastic Systems, Springer-Verlag, 1960.
[21] Y. Öngün, M. André, D. Bartel, L. Deters, An axisymmetric hydrodynamic interface element for finite-element computations of mixed lubrication in rubber seals, Proc. Inst. Mech. Eng. J. J. Eng. Tribol. 222 (2008) 471–481.
[22] S. Stupkiewicz, A. Marciniszyn, Elastohydrodynamic lubrication and finite configuration changes in reciprocating elastomeric seals, Tribol. Int. 42 (2009) 615–627.
[23] D. Shen, R.F. Salant, An unsteady mixed soft EHL model, with application to a rotary lip seal, Tribol. Int. 40 (2007) 646–651.
[24] L.E.C. Ruskell, A Rapidly Converging Theorectical Solution of the Elastohydrodynamic Problem for Rectangular Rubber Seals, Proc. Inst. Mech. Eng. J. Mech. Eng. Sci. 22 (1980) 9–16.
[25] G.K. Nikas, R.S. Sayles, Computational model of tandem rectangular elastomeric seals for reciprocating motion, Tribol. Int. 39 (7) (2005) 622–634.
[26] G.K. Nikas, R.S. Sayles, Study of leakage and friction of flexible seals for steady motion via a numerical approximation method, Tribol. Int. 39 (2006) 921–936.
[27] M. Flamant, Equilbre d'elsaticite–sur la reparitition des pressions dans un rectangulaire change transversalement, C.R. Acad. Sci. Paris 114 (1892) 1465.
[28] R. Gohar, H. Rahnejat, Fundamentals of Tribology, Imperial College Press, London, 2008.
[29] D. Jalali-Vahid, H. Rahnejat, R. Gohar, Z.M. Jin, Prediction of Oil-film thickness and shape in elliptical point contacts under combined rolling and sliding motion, Proc. Inst. Mech. Eng. J. J. Eng. Tribol. 214 (2000) 427–437.
[30] J.A. Greenwood, Film thicknesses in circular elastohydrodynamic contacts, Proc. Inst. Mech. Eng. C. J. Mech. Eng. Sci. 202 (1988) 11–17.
[31] J.R. Seth, R.T. Bonnecaze, Influence of short-range force on wall-slip in microgel pastes, J. Rheol. 52 (2008) 28.